

1   **Application of Structural Identification and Non-Destructive Evaluation Techniques**  
2   **to Diagnose Root Causes of Bridge Performance Problems**

3   *J. Weidner, F.L. Moon, N. Gucunski and A. E. Aktan.*

4   **Abstract**

5   *For nearly fifty years, visual inspection has served as the foundation of bridge assessment. This*  
6   *is effective for determining bridge condition at a low resolution, but diagnosing root causes of*  
7   *performance issues generally requires quantitative information. This paper describes a part of*  
8   *the International Bridge Study (IBS). The IBS effort brought researchers from around the globe*  
9   *to a single, typical highway bridge in the United States to demonstrate best practices of bridge*  
10   *assessment. The focus of this paper is on the Structural Identification and Nondestructive*  
11   *Evaluation (NDE) conducted by Drexel University and Rutgers University, respectively. A*  
12   *comprehensive instrumentation plan for static truck testing was developed based on rigorous*  
13   *finite element model simulations. The bridge was load tested using six triaxle dump trucks. The*  
14   *bridge deck was comprehensively assessed using a variety of NDE techniques as well. The load*  
15   *test data and NDE data were assessed independently, collectively and through finite element*  
16   *calibration. Bridge conclusions about loss of composite action, deck delamination, bearing*  
17   *performance, fatigue cracking, and unexpected non-linear behavior of a single girder are*  
18   *presented. Many of these conclusions were only possible through a multi-modal assessment*  
19   *approach with the goal of identifying root causes of performance issues.*

21    **Introduction**

22    The corner stones of bridge assessment in the U.S. are visual inspection per the National Bridge  
23    Inspection Standards (NBIS) and load rating according to the American Association of State  
24    Highway Transportation Officials (AASHTO) Manual for Bridge Evaluation. Depending on the  
25    importance of the bridge and the complexity of its real or perceived deficiencies, these traditional  
26    methods may be complemented by technology applications like nondestructive evaluation (NDE)  
27    and load testing, structural identification (St-Id) and structural health monitoring (SHM). In  
28    addition to the inertia of the profession, the cost, time, and expertise required to adapt and  
29    implement such technologies in a meaningful way within the realm of bridge engineering  
30    practice has slowed their use. This paper, intended as a companion to a forum paper (Moon et al.  
31    2015), discusses how a highway bridge with a multiplicity of complex, interacting damages and  
32    deterioration was leveraged to demonstrate how the principles recommended in the Forum paper  
33    were applied successfully to identify the root causes of damage and deterioration.

34    To understand and document both the state-of-the-practice and the state-of-the-art related to  
35    technology-enabled bridge assessment (and how these vary around the world), a unique study,  
36    termed the International Bridge Study (IBS), was conceived during the Pilot Phase of the Federal  
37    Highway Administration's Long-Term Bridge Performance Program (FHWA 2015). The  
38    overarching objective of the IBS was to formulate and demonstrate best practice approaches for  
39    the integration and application of technology to diagnose, perform prognosis, and design  
40    treatments to mitigate performance deficiencies of common highway bridges. As part of this  
41    program, an operating multi-girder bridge in the eastern U.S. (which displayed a variety of  
42    common performance deficiencies) was selected to serve as a field laboratory. Seventeen teams  
43    of experts from the U.S., Europe and Asia visited the bridge and made observations,

44 conceptualized its performance, and hypothesized potential root causes of any identified  
45 deficiencies. These teams then performed a series of assessments (through visual inspection,  
46 dynamic monitoring, controlled dynamic testing, controlled load testing, St-Id, and various forms  
47 of NDE) to identify the root causes of deterioration, assess their impact on performance, and  
48 ultimately develop mitigation strategies. Examples of these applications include Su et al. (2011),  
49 Pasquier and Smith (2015), Zhang et al. (2013), Sigurdardottir and Glisic (2014), Veggeberg  
50 (2013), Wenzel et al. (2011), Zhu et al. (2011) and Zhou et al. (2012). In addition, it is  
51 envisioned that the test bridge, having been thoroughly dissected and documented, will be an  
52 ideal test bed for demonstrations, field calibrations, and validations of emerging technologies in  
53 the future.

54 As the full depth of the IBS study is beyond the scope of a single journal paper, this paper will  
55 focus on the St-Id effort executed by Drexel University and the NDE deck assessment carried out  
56 by Rutgers University. In particular, the goals of this paper are to provide (a) a detailed  
57 documentation of these applications and the principles that guided them, and (b) an example of  
58 how disparate, multi-modal data may be integrated to quantify and understand both poor bridge  
59 performances, and their respective root causes.

## 60 **Bridge Description**

61 The test bridge is located in the eastern U.S. and is part of a four span steel, multi-girder bridge  
62 built in 1983. This bridge while less than 30 Years old, was identified by the owner as a good  
63 candidate for the IBS since it displayed many common performance problems with uncertain  
64 root causes. The bridge was not structurally deficient, functionally obsolete, or posted for any  
65 load restrictions. The overall geometry of the structure is shown in Figure 1 and the

66 superstructure is shown in Figure 2. Due to the unfettered access to its underside, Span 2SB was  
67 selected as the primary focus of this study. The following bullets provide salient details of the  
68 structure:

- 69 • Network and Utilities: The test bridge is located on a feeder highway to a major city and  
70 carries 90,000 vehicles a day with 4% truck traffic. The bridge spans roadways (Spans 1  
71 and 4), a railroad (Span 3) and a pair of buried, 1.83 m (72 in.) diameter water mains  
72 (Span 2). The bridge also carries a natural gas line in the first bay along the west side.
- 73 • Superstructure (Span 2SB): Viewed in plan, this span is a right trapezoid with the skewed  
74 side at an angle of 24° relative to the transverse axis. The length of the span is 39.6 m  
75 (130 feet) on the long side and 32 m (105 feet)) on the short side. The out to out width is  
76 19.0 m (62.25 feet). The superstructure of the bridge is composed of eight built-up  
77 girders with 1.52 m (60 inch) deep webs and variable thickness flanges (ranging from  
78 25.4 mm (1 inch) to 51 mm (2 inches)), a composite reinforced concrete deck, and X-  
79 framed diaphragms spaced at 6.6 m (21.7 ft.).
- 80 • Substructure and Bearing: The bridge is supported by steel rocker bearings along the  
81 skew end and pinned bearings along the straight end. The bearings under the fourth girder  
82 have 1.5 mm (1/16 in.) lateral movement allowance (so-called alignment bearings),  
83 whereas all other bearings have 3 mm (1/8 in.) lateral movement allowance. The bearings  
84 are supported by a 1.52 m (5 ft.) deep reinforced concrete pier cap that spans four 1.22 m  
85 (4 ft.) diameter reinforced concrete columns.
- 86 • Condition and Qualitative Performance Assessment: Visually, the deck appeared to be in  
87 good condition, given the presence of periodic full-width transverse hairline cracks, and  
88 some sporadic spalling. There was a large bump noted in the driving surface at the

89 interface between the approach slabs and the first span of the bridge. The bump tended to  
90 excite vehicle traffic, particularly trucks. On the northbound side a loss of fill under the  
91 sidewalk and approach slab resulted in settlement. The girders were in generally good  
92 condition except for the presence of fatigue cracks at the webs of exterior girders at the  
93 wind brace to girder web connections (the most recent inspection report noted 80 such  
94 cracks). The rubber deck expansion joint fillers were in poor condition, often partially  
95 missing, or filled with debris. The exterior bearings were heavily deteriorated, while the  
96 interior bearings were in better condition. One external bearing was observed to have  
97 broken the pintel (which holds the bearing in place) and rotated approximate 20° about  
98 the vertical axis. The substructure was in fair condition, with evidence of corrosion,  
99 delamination and efflorescence on the pier caps. In particular, a large diagonal crack that  
100 ran between the bearing of the exterior girder and the first supporting column (Figure 2)  
101 was noted on Pier 1S (Figure 1). Finally, all research teams and the past inspection  
102 reports noted that the bridge exhibited “lively” vibrations under normal traffic.

### 103 **Overview of Structural Identification**

104 The Paradigm of Structural Identification (St-Id) aims to develop reliable estimates of the  
105 performance and vulnerability of structural systems through the integration of simulation models  
106 with qualitative observations and quantitative response data. The St-Id paradigm for civil  
107 infrastructure was initially developed by Liu and Yao (1978). Recently it was formalized in an  
108 ASCE State-of-the-Art Report (Catbas et al. 2013), and is discussed in greater detail in the  
109 accompanying forum paper (Moon et al. 2015). Figure 3 provides a summary of the St-Id  
110 process, a framework to guide and structure the integration of disparate sources of information in  
111 order to answer questions critical to understanding the behavior of the bridge. It is stressed that

112 while the St-Id process provides a sound structure with which to implement technology for  
113 assessment, it does not remove requirements for multi-disciplinary expertise, best practice  
114 modeling and data collection approaches, and sound heuristics.

115 As shown in Figure 3, the first step of St-Id involves conceptualizing the structure together with  
116 the concerns and issues that are driving the application. Although this step does not necessarily  
117 employ any advanced technologies, it has more influence over the ultimate success of the St-Id  
118 than any other as it develops the guiding questions/objectives. The second step of the process  
119 involves developing an a priori model to ascertain the uncertain mechanisms that most  
120 significantly influence the performances of interest. The third step both designs and carries out a  
121 testing/data collection campaign to acquire the data necessary to reduce the uncertainty  
122 associated with these mechanisms. Data processing, error screening, reduction, and interpretation  
123 is handled in Step 4 to put the data in a useable form and ensure quality. Step 5 aims to reconcile  
124 the simulation model (often from Step 2) to the acquired data through manual (Friswell et al.  
125 1998, Brownjohn et al. 2001, Daniell and Macdonald 2007), deterministic (Friswell et al. 2001,  
126 Robert-Nicoud et al. 2005) or probabilistic (Beck and Katafygiotis 1998, Beck 2004, Dubbs and  
127 Moon 2015) updating techniques to better identify the uncertain and influential mechanisms. The  
128 final step of the process involves using the calibrated model through scenario analysis,  
129 parametric studies, or what-if simulations, to inform the guiding questions.

130 Observation and Conceptualization

131 The conceptualization of the IBS Bridge involved gathering and reviewing relevant  
132 documentation that included drawings, photographs, past load rating reports, inspection reports,  
133 etc. This was followed by site visits and face-to-face discussions with the bridge owner. To  
134 better quantify the perceived lively vibrations, a cursory ambient vibration survey was

135 conducted. This survey found that under normal operating conditions the acceleration amplitudes  
136 associated with the fundamental mode of vibration was routinely on the order of 0.3 g. Note that  
137 there were numerous observations which did not lend themselves to technology application. For  
138 example, the presence of the gas line poses a hazard to the bridge, and subpar drainage may have  
139 led to premature deterioration but these are not quantifiable, highlighting the need for expert  
140 heuristics as well as structural identification. To address these structural performance concerns, a  
141 series of critical questions were formulated as follows:

- 142 (1) What is the root cause of the observed, evenly spaced, transverse deck cracking?  
143           What is the effect of these cracks on the long-term durability of the deck?
- 144 (2) What caused the formation and propagation of the existing fatigue cracks?
- 145 (3) What caused the rotation of the exterior rocker bearing? Does the span geometry play  
146           an additional role?
- 147 (4) What is the root cause of the diagonal crack in the pier cap? Does this crack indicate  
148           any potential safety issues?
- 149 (5) What was the root cause of the observed “bump” at the end of the bridge?

150 A Priori Modeling

151 The a priori model provided estimates of structural responses which were used to (1) specialize  
152 the specific experimental approaches selected (sensor layout, load levels, etc.), and (2) ensure  
153 safety and provide a comparison point for real-time interpretation of data during the experiment.  
154 The actual modeling approaches adopted depended on the objectives of the St-Id as well as the  
155 complexity of the structural system and its behaviors identified. The focus of the IBS study was  
156 on load carrying mechanisms and load path, vibration characteristics and overall structural  
157 behavior, which indicated that a structural model (element-level model) would be appropriate as

158 the primary a priori model. This type of model generally employs a combination of frame  
159 elements (to simulate beams and columns), shell elements (to simulate slabs and walls), and link  
160 elements (to permit the 3D geometry to be approximated). The model developed for this study  
161 focused only on Span 2 SB and did not include the piers, the crown of the roadway, the vertical  
162 curvature of the span, or the effects of the adjacent spans. To verify that these simplifications did  
163 not alter the simulation of key responses, a series of parametric studies were carried out. Weidner  
164 (2012) provides details of these studies for the interested reader.

165 During the construction of the model, error screening at various levels of completeness was  
166 carried out by examining the model for: (1) duplicate nodes and members, (2) plausible deflected  
167 shapes under dead load and simple live load patterns, (3) physically consistent mode shapes, (4)  
168 local compatibility, and (5) local and global equilibrium. The final model was comprised of 5072  
169 elements, including 1469 beams, 2535 plates and a 1068 link elements. The typical element  
170 dimension size was 61 cm (24 in.) for primary elements. The model is shown in Figure 5.  
171 Schematic examples of the bearing to girder connections in the model can be seen in Figure 6.

172 The St-Id framework explicitly divides A Priori modeling and Experiment into separate steps,  
173 but in reality the process of designing the experiment (instrumentation layout, load requirements,  
174 etc.) makes use of the model. The model combines bridge engineering experience and heuristics  
175 with modeling knowledge. Through parametric studies, the model becomes a valuable tool for  
176 exploring whether and how various mechanisms may influence the performances/responses of  
177 interest (as defined by the guiding questions). This information is key to the development of an  
178 efficient and effective instrumentation and testing plan, as it allows the modality, spatial location,  
179 and resolution of responses that are relatively sensitive to the mechanisms of interest and  
180 relatively insensitive to inconsequential mechanisms.

181 The goal was to verify (1) the responses are sensitive to variation in the parameters and (2) the  
182 response magnitudes were sufficiently beyond the noise threshold of the sensor. For the IBS  
183 study, three preliminary (pre-test) parameters (together with their bounds) were identified as  
184 representative of the uncertainties related to the guiding questions (see Table 3). An automated  
185 modeling process was developed using MATLAB and Strand7 which generated a large set of  
186 parameter values, executed the model analyses with each parameter set, and extracted and  
187 processed the results. The parameters were sampled using a Monte Carlo approach assuming a  
188 uniform distribution between the bounds. The results of this study, and their use within the  
189 instrumentation design process, are discussed in the following section.

190 Experiment Design

191 Addressing the critical questions required that the force-resisting mechanisms and  
192 boundary/continuity conditions were established, which necessitated capturing the full transfer  
193 function (e.g. input-output relationship). As such, the primary focus was a controlled live load  
194 test by six tri-axle dump trucks of measured wheel-weights (where input was known) and non-  
195 destructive testing of the deck. Beyond that, ambient monitoring of traffic and vibration  
196 monitoring were also included. While different teams from Drexel and Exeter performed MIMO  
197 dynamic tests, these are not discussed here.

198 Instrumentation utilized for the static load test was designed to: (1) stay within test constraints,  
199 (2) satisfy the overall test objectives and (3) provide the user with situational awareness to  
200 maintain safety and assess/correct any data quality issues that may arise during the experiment.

201 The primary constraints for this test included the railway right-of-way, the height of the span  
202 (which precluded ladder access), the high ADT (which limited top-side access), the lack of

203 power available on-site, and budget and time constraints that allowed for purchase, installation,  
204 and acquisition of approximately 100 channels of data. The budget allowed for the purchase of  
205 60 sensors including primarily strain gages and potentiometers, as well as the data acquisition  
206 system. The remaining sensors, including additional strain gages, crack gages, and linear variable  
207 displacement transducers came from existing stock at Drexel University. Though the bridge was  
208 visited several times throughout the project, time on site, and in turn instrumentation, was limited  
209 by budgetary requirements for traffic control and logistical costs (i.e., travel expenses).  
210 Considering these constraints, a core instrumentation layout was developed and revised by  
211 varying critical model parameters and investigating the influence of these parameters on  
212 response magnitudes at the instrument locations.

213 Figure 7 shows the response prediction histogram for displacement at mid-span of Girder #3.  
214 These plots were developed and assessed at all potential instrumentation locations to verify the  
215 sensor requirements (sensitivity and magnitude) were met.

216 Following refinement and verification of the instrumentation layout, the final instrumentation  
217 plan was developed as shown in Figure 8. The primary sensors were clustered into a grid of  
218 twelve sensor node locations. Each node contained a Celesco PT8510 displacement sensor, and  
219 at least two HiTec Products weldable strain sensors with a two inch shim length and a 0.5 inch  
220 gage length. The displacement transducers were mounted to a plate, clamped to the underside of  
221 the bottom flange, and referenced to the ground via high strength fishing line connected to a  
222 weight. Figure 9 shows the typical longitudinal configuration of strain gages. This configuration  
223 consisted of two, or at select locations, three gages at the same longitudinal distance from the  
224 bearings. The first was mounted on the topside of the bottom flange and the second was mounted  
225 50.8 cm (20 inches) up the web to allow the strain profile and the level of composite action at the

226 cross section to be estimated. In a few locations a third strain gage was added to allow the  
227 linearity of the strain profile to be assessed. Although it was desirable to have strain and  
228 displacement sensors on every girder at a given line to permit the direct extraction of distribution  
229 factors, budget constraints made this impossible. Since one of the key response mechanisms to  
230 be examined was the level of composite action, multiple sensors at each cross-section were  
231 required and thus only a subset of the girders could be instrumented. A more detailed  
232 description of the complete instrumentation program can be found in Weidner (2012).

233 A distributed data acquisition network was used, employing five independent nodes spread  
234 across the superstructure and networked with Ethernet cable. This provided flexibility for cable  
235 routing, and reduced the overall length of cabling required substantially. The location of the five  
236 data acquisition nodes are shown in Figure 8.

237 Table 1 maps the designed instrumentation plan to the critical questions via data relationships.  
238 To facilitate situational awareness, many of these relationships were included in a data  
239 visualization portal. The data visualization portal (Figure 10) was developed to interface with the  
240 data in real-time during testing. This portal included data acquisition control, network  
241 connectivity, and traditional response time history plots. In addition, the portal utilized higher  
242 order plots which presented data in a relational sense, taking advantage of the fixed spatial  
243 relationships between sensors. In other words, rather than viewing a time history of all  
244 displacement sensors on a single plot, the response values were plotted along girder lines,  
245 effectively showing a displaced shape for the girder. This facilitates intuitive interpretation of the  
246 data in real-time.

247 Experiment Execution

248 The live load test of Span SB2 was carried out between 4:30 AM and 8:50AM. During this entire  
249 window two of the three lanes were closed to traffic, with complete closure of all lanes when  
250 required by the load case. The weather during the test was clear with humidity ranging from 70%  
251 to 40% and with temperatures ranging from 75° F to 48° F.

252 Six trucks with three rear axles (one retractable) were made available by the bridge owner. This  
253 allowed for three load stage levels, up to a final load stage consisted of six fully loaded trucks  
254 with total weight of approximately 2046 kN (460 kips). For each loading scenario, a series of  
255 simulations were carried out to identify the likely bounds (through the sampling of the  
256 parameters shown in Table 2) of each of the response measurements. This permitted the rapid  
257 assessment of both data quality and bridge performance in near-real time as each channel could  
258 be readily compared against its estimated bounds identified through simulation.

259 Note that this loading scheme was not geared towards a particular rating or scenario, but rather  
260 aimed at identifying how the uncertain and influential mechanisms (related to the guiding  
261 questions) actually perform. To satisfy the overarching objective of understanding the potential  
262 root causes of the identified performance problems, the structural characteristics related to load  
263 path, stiffness, linearity, compatibility and boundary conditions had to be established. As a result,  
264 the entire effort was necessarily more open ended than a load rating exercise, and thus demanded  
265 a series of loading scenarios with different magnitudes and spatial distributions.

266 Data Reduction

267 Static and crawl truck testing along with ambient traffic monitoring produced substantial  
268 amounts of data. Reducing this data and extracting valuable information from it required a sound  
269 approach to both preparation of the data and the relationships within the data that are considered.

270 Data preparation for static truck testing is straightforward. This consists of identifying time  
271 windows of interest, removing any offsets or biases, averaging response magnitude and  
272 tabulating the results. The tabulated strain and displacement results for the final load case are  
273 presented in Table 3. Weidner (2012) provides a comprehensive documentation of all load cases  
274 for the interested reader.

275 Table 1 shows the spatial and multi-modal data relationships that were used to investigate the  
276 critical questions identified previously. These relationships are often good indicators of  
277 performance as the behavior can be expected to fit a certain form informed by heuristics. Figure  
278 11 shows the girder displacement profiles along the four instrumented girders under the full load.  
279 The behavior of Girder #1 can clearly be seen as an outlier as compared to the other girders. This  
280 is discussed in more detail later in this paper.

281 Model-Experiment Correlation

282 The a priori model, along with several subsequent iterations were both manually and  
283 automatically calibrated considering the experimental data. Manual calibration consisted of  
284 adjusting parameter values based on an expected influence on the model, generally one at a time,  
285 and executing the model analysis, extracting results, and comparing to the experimental value.  
286 The goal of this approach was to identify a set of parameter values which adequately represented  
287 the experimental behavior. Although labor intensive, this process allows the user to explore the

288 parameter space with more freedom and helps the development of heuristics and intuition about  
289 the bridges performance.

290 Automated calibration, or parameter identification, consists of minimizing the sum of the square  
291 of the errors between experimental and analytical responses via an objective function. The  
292 optimization algorithm used here was LSQNONLIN in Matlab, which takes advantage of the  
293 trust-region-reflective algorithm. This algorithm allows for parameter boundaries, which is  
294 critical when parameters have physical or realistic bounds. However, the problem cannot be  
295 underdetermined, meaning the number of parameters was limited. The problem was reduced via  
296 combining parameters where appropriate, like boundary stiffnesses, to converge on a smaller set  
297 of parameters. Each iteration of the automated calibration started with a new set of initial  
298 parameter values to help mitigate the influence of local minima.

299 Table 4 presents the experimental results and calibrated analytical results for displacement and  
300 strains using both manual and automated calibration. The manual calibration was executed  
301 considering both displacement and strain data simultaneously. The automated calibration was  
302 executed using both, as well as two alternate cases considering each response modality  
303 independently. Automated calibration using only displacement data resulted in a final model that  
304 can adequately represent both modalities. In fact, the results were similar to the automated  
305 calibration using both strain and displacement. Automated calibration using only strain data did  
306 not produce a final model with the same order of magnitude of accuracy for either modality. This  
307 is attributed to the fact that the strain responses were not overly sensitive to changes in the  
308 selected parameters.

309 As a final check on the validity of the calibrated models, a final automated calibration was  
310 executed including a parameter commonly accepted as deterministic, the modulus of the steel  
311 girders. Any dramatic shift of this parameter would be an indicator of the inadequacy of the  
312 model to represent the experiment, as it would essentially be violating what is known to be true.  
313 The modulus varied within 1% of the accepted value of 199 GPa (29,000 ksi). Other data sets  
314 were available for validation, including dynamic properties, but these are beyond the scope of  
315 this current paper.

316 Table 5 presents the parameter values corresponding to those two calibrated models (manual and  
317 automated). Recall that the number of parameters had to be reduced, necessitating the  
318 combination of certain parameters, like composite action and bearing stiffnesses, which were  
319 split during manual calibration.

320 Additionally, multiple model methods were explored including techniques to allow the  
321 optimization to select between alternate model forms (i.e., beam-shell or full shell construction).  
322 This subject is beyond the scope of this paper, and will be discussed in subsequent papers. More  
323 details about the calibration efforts, the final calibrated results, and multiple model approaches  
324 are presented in Weidner (2012).

325 The model and structural testing data, together with the NDE results (described in the following  
326 section) were integrated to evaluate several performance deficiencies. The results of this  
327 integration are presented following the NDE results. The interested reader is directed to Weidner  
328 (2012) for a complete accounting of all simulation-related investigations conducted on the IBS  
329 test bridge.

330 **Nondestructive Evaluation of the Deck**

331 An NDE survey consisting of six technologies: impact echo (IE) survey to detect and  
332 characterize delamination, electrical resistivity (ER) to describe the corrosive environment and  
333 the expected corrosion rate, half-cell potential (HCP) to assess the probability of active  
334 corrosion, ultrasonic surface waves (USW) method to measure concrete modulus, the ground  
335 penetrating radar (GPR) to measure concrete cover and provide a qualitative deterioration  
336 assessment, and microwave technology MoistScan to detect areas of higher moisture content.  
337 The NDE survey was conducted on a 0.61 m. (2 ft.) by 0.61 m. (2 ft.) grid. The origin of the  
338 coordinate system was the intercept of joints that bound span 1 and 2, and the curb. The first  
339 survey line was one foot away from the curb. All the technologies took measurements at all grid  
340 points. The exception was the USW measurement, which was conducted on a 1.21 m. (4 ft.) by  
341 1.21 m. (4 ft.) grid.

342 As described earlier, each of the technologies excels in detecting and characterizing one of the  
343 deteriorating conditions. The results of the survey are presented in Figure 12 through Figure 18.  
344 For all NDE method results, except the moisture content measurement, the hot colors (reds and  
345 yellows) represent a high level of deterioration or lower quality for USW, and the cool colors  
346 (blues and greens) indicate a low level of deterioration or good condition. Both the HCP and ER  
347 results point to low probability of corrosion activity and low corrosion rate, respectively. One of  
348 the possible reasons is a lower moisture content, as qualitatively described through the Moist  
349 Scan measurement. (It should be noted that the Moist Scan measurement provides a relative  
350 moisture content measurement. The absolute value should be obtained through calibration with  
351 cores or other approaches.) A similar assessment was obtained from the GPR measurement,  
352 which effectively describes the corrosive environment of concrete. In addition, some areas of

353 low resistivity from ER measurements and higher attenuation in the GPR survey (Figure 14)  
354 correlate well. The GPR survey (Figure 13) also points to variability of the concrete cover from  
355 less than five cm (two inches) to more than ten cm (four inches) at some locations.

356 Results of the USW measurement, shown in Figure 18, point to a low strength concrete,  
357 considering that the measured modulus was mostly in a 13.8 to 27.5 GPA (2000-4000 ksi) range.  
358 This was later confirmed through review of design plans, which specified a “low modulus”  
359 concrete for the deck. Finally, results of the IE delamination assessment, shown in Figure 16,  
360 point to a significant number of delaminations in the deck. This is somewhat surprising,  
361 considering the low corrosion activity measured by HCP and fair corrosive environment obtained  
362 from ER.

363 **Data Integration and Analysis**

364 A unique component of the IBS was that it provided the opportunity to explore the potential  
365 benefits of multiple modalities of data. Often when structures are field tested, particularly in  
366 support of determining load ratings, instrumentation is limited to a single modality, mainly strain  
367 gages. IBS included not only multiple modalities of sensor data, but also a comprehensive NDE  
368 evaluation of the deck. These data sources were manually used together in order to draw specific  
369 conclusions about the performance of the structure. This is not data fusion in the traditional  
370 sense, as the data were not fused automatically via an algorithm or other technique. Rather, this  
371 is considered manual data integration. This is equally important during testing, where systemic  
372 biases (data acquisition errors, for example) may skew responses for every single sensor of a  
373 given type. Data integration is a critical tool for corroborating data sets because each data set is

374 subject to its own uncertainties and systemic errors. Data integration across multiple modalities  
375 of response provides the user with context and perspective.

376 Softness of Girder #1

377 Figure 19 shows displacement of all four girders at the  $\frac{1}{4}$  point with the load positioned at the  
378 same point. It is evident that as the load increased, Girder #1 showed substantial non-linear  
379 behavior (softening). Some apparent softening was seen throughout the test at all directly loaded  
380 locations, as shown in both displacements at midspan with the load at midspan (shown in Figure  
381 20) as well as strains at the same location and loading (shown in Figure 21). This typical  
382 behavior was attributed to changes in load configuration (three trucks versus six trucks, back to  
383 back) at higher load levels and was much less pronounced than the behavior of Girder #1 at the  
384  $\frac{1}{4}$  point. Figure 14 shows the strain behavior at that position and load level, which give no  
385 indication of softening beyond the typical behavior. Considering these two responses together, it  
386 is clear that at the highest load level, Girder #1 experienced a vertical translation of one of its  
387 supports. A support settlement would directly manifest in displacement response, but only  
388 indirectly observed through strain responses if the support movement results in a re-distribution  
389 of forces. Given that the observed displacement response was isolated to Girder #1, it was  
390 determined that it was a result of the crack in the piercap near Girder#1 (shown in Figure 3).

391 To highlight the importance of multi-modal instrumentation and data integration, consider a  
392 typical diagnostic load test used to update load ratings. Instrumentation for this test would likely  
393 be only strain gages, as these can be used, per the AASHTO MBE, to scale load ratings based on  
394 the proportional increase in strain measure experimentally versus analytical estimates. To  
395 simulate this scenario, an automated calibration of the model using only strain data was  
396 executed. By excluding the displacement information from the calibration effort, it is possible to

397 simulate the experiment without displacement. In this case, the calibrated model was entirely  
398 incapable of predicting displacements or strains very well, as the parameters were not as  
399 influential on strain response. The comparison of experimental and analytical displacements and  
400 strain from a model calibrated using only displacement data are presented in Table 6.

401 Deck Delaminations

402 IE testing indicated that there were delaminations present in the concrete deck of Span 2 of the  
403 IBS bridge. However, these delaminations were identified in areas with only minor indications of  
404 corrosion. These findings indicate that the expansion of corroding rebar was likely not the cause  
405 of the observed delaminations. This notion of delamination without a highly corrosive  
406 environment is corroborated by findings from the tests conducted by Drexel University.

407 From the static truck testing, areas of apparent loss of composite behavior were identified. Figure  
408 24 shows the strain profile of Girder #1 and Girder #3 at the three-quarter point, with load  
409 directly above at maximum level. Girder #1 appears to be behaving compositely while Girder #3  
410 is almost completely non-composite. These instrumented cross-sections correlate to locations  
411 where NDE assessment indicates that delaminations were present and the concrete modulus was  
412 low, but the corrosive environment in the concrete was minimal.

413 Alampalli (2001) hypothesized that deterioration in the concrete deck of many bridges in the  
414 state of New York may have resulted primarily from vibration related issues. This is a plausible  
415 explanation for the deterioration at the IBS Bridge. As was noted earlier, the span felt lively to  
416 humans on the bridge, and under normal traffic, peak accelerations of 0.3g were common.  
417 Ambient traffic monitoring supported the observation of heavy span vibration experienced both  
418 under traffic load and truck loads. Figure 25 shows a 20-second window of time including three

419 major truck events and normal traffic in-between. After the first truck, which has a large static  
420 component, the vibration response damps out fairly quickly. The bridge is then rapidly excited to  
421 a brief period of resonance under normal traffic loading. The response magnitude in this period is  
422 far greater than would be expected based on the static weight of traffic as compared to the truck.

423 Though it is not possible to eliminate construction-related issues as a driver for this deterioration,  
424 the fact that the bridge has been experiencing large magnitude, nearly symmetric vibrations  
425 under normal traffic for its entire life are a likely cause. These vibrations can and would have put  
426 the deck into tension, and caused delaminations and general deterioration.

427 Bearing Performance

428 Recall that the IBS Bridge was supported on steel rocker bearings, which exhibited several  
429 performance problems. The calibrated model was used to run a simple simulation to understand  
430 how the structure would naturally deform if the expansion bearings did not have any lateral  
431 restraint. When subjected to a uniform temperature increase, the bearings tended to move in a  
432 direction approximately  $71^\circ$  from their designed direction of movement. Under standard live  
433 load, the bearings tended to move in a direction approximately  $-55^\circ$  from the design direction of  
434 movement. This can be seen in Figure 26. Given that the bearings were restrained laterally, this  
435 behavior provides an explanation for the deterioration and cracking found in the bearing pintels.

436 Fatigue Cracking

437 The fatigue cracking at the connection detail between the wind bracing and the two girders  
438 comprising the exterior bays was investigated. The ADTT of the structure does not exceed the  
439 theoretical infinite fatigue life, meaning that the presence of the fatigue cracks must result from  
440 one or more other mechanisms. Using strain measurements taken from ambient traffic data sets

441 collected while on site, the stress range was approximated at 19.8 MPa (2.87 ksi), which  
442 corresponds to a fatigue life of 46.7 years. Static testing and ambient monitoring showed  
443 substantial differential displacement between girders, likely due to the geometry of the span. As  
444 a result of this differential displacement, it is believed that the wind bracing was distorting the  
445 web out-of-plane at the connection detail. This detail was located close to the bottom flange and  
446 a vertical stiffener, resulting in an area of local distortion stress. Using the model, an analysis  
447 scenario was run to compare the behavior of the bridge with and without the wind bracing, which  
448 was primarily used for construction stability. It was shown that the bracing could be removed  
449 without consequence to the performance of the bridge, which would prevent the development of  
450 additional fatigue cracks.

451 Load Rating Application

452 While the IBS Bridge did not have a capacity issue, and was not posted, the calculation of load  
453 ratings is still an informative exercise about St-Id as a tool for load rating of problematic bridges.

454 Table 7 shows a summary of flexural load rating (Inventory) values of various models, as well as  
455 the rating provided by the Bridge Owner. The model-based ratings are applicable to midspan of  
456 Girder #4, which was an assumed location based on common practice for sensor installation (i.e.,  
457 midspan of girder will see maximum response). The inspection report only presents the  
458 controlling flexural rating, which applied to Girder #5. The original model corresponds to a  
459 refined analytical load rating, while the manual calibrated, statically-calibrated and dynamically-  
460 calibrated models are based on the experiment. Through experimentation and model calibration,  
461 the ratings for this structure were improved. This improvement is attributed primarily to better  
462 lateral distribution of load than is assumed in a single line girder approach.

463 Other Performance Issues

464 The cause of the movement of sidewalks and approach slabs, and the resulting “bump” at the end  
465 of the bridge were a major question for the IBS Investigation. This type of performance issue is  
466 difficult if not impossible to identify and explain through instrumentation and technology.  
467 Through heuristics and field observations, it was concluded that blocked drainage and joint  
468 failure resulted in water washing out fill beneath the sidewalk and approach slabs, causing  
469 settlement. Though not directly influencing Span 2 SB, which was the focus of most of this  
470 effort, the presence of a bump at the end of the bridge which accelerates bridge deterioration is a  
471 critical performance issue.

472 **Conclusions**

473 This paper introduces the International Bridge Study as a field research effort aimed at bringing  
474 bridge assessment expertise from around the world to a single test specimen. A common bridge,  
475 yet a unique test specimen, with an uncommon multiplicity of performance deficiencies was  
476 selected in the Northeastern portion of the United States. Experts both domestic and  
477 international, particularly European and Asian, traveled to the bridge to demonstrate  
478 technologies and practices native to their regions. To serve as a baseline reference, Drexel  
479 University conducted a full structural identification via load testing. Similarly, Rutgers  
480 University carried out a comprehensive evaluation of the deck using nondestructive techniques.  
481 This paper focuses on the results from these two studies in particular.

482 Through the integration of these disparate data sources, three primary performance issues were  
483 quantified, and the root cause of the issues were identified. First, through the comparison of  
484 strain and displacement data, a non-linear response in the exterior girder of the tested span was

485 identified. This finding was supported through the use of model calibration. The root cause of  
486 this behavior was a crack in the piercap, which was shown to be active through targeted  
487 instrumentation over the crack. Subsequent review of the documentation for the structure  
488 indicated that rebar in the top of the piercap was likely not fully developed. This behavior point  
489 to a critical design error and would not have been identifiable with strain information only.

490 Second, the comprehensive evaluation of the deck using nondestructive testing identified regions  
491 of delamination throughout the bridge that were not associated with active corrosion in the deck.  
492 The deterioration did correspond to areas where a loss of composite action was identified via  
493 strain measurements during the load test. The root cause of the delamination was determined to  
494 likely be excessive vibration of the deck due to vehicular loading. Dynamic behavior of the semi-  
495 skew superstructure was observed to amplify the truck responses and oscillate the deck  
496 substantially. The vibration was due to the tendency of the bridge to resonate under the input by  
497 traffic, and points to a need to explicitly consider traffic excitation and vibration during the  
498 design of such irregular structures.

499 Finally, the fatigue cracks were determined to be a result of distortion induced fatigue. Though  
500 the retrofits appeared to keep the crack propagation in check, analysis showed that the problem  
501 could be better mitigated by removing the wind bracing which was determined to not be critical  
502 for the functionality and the safety of the span in its current configuration.

503 Structural identification was demonstrated as key to answer common problems (i.e., load ratings)  
504 and also the causes of more complex performance issues. The IBS demonstration shows the  
505 importance of considering multiple data sources when using structural identification to identify  
506 the root cause of structural performance issues. This effort exemplifies the concepts put forth in

507 an accompanying forum paper (Moon et al. 2015) which generally state that standard assessment  
508 practices are not conducive to determining root causes of deterioration or poor performance.  
509 Instead, an experiment targeted at addressing specific questions must be designed and executed  
510 with a focus on validating or disproving these hypotheses. St-Id provides a solid framework to  
511 achieve these goals by guiding an integrated application of heuristics with sensing, information,  
512 simulation and decision technology tools.

513 **Acknowledgements**

514 The authors would like to acknowledge the support and assistance from the Rutgers Center for  
515 Advanced Infrastructure and Transportation (CAIT), the Federal Highway Administration and  
516 the Long-Term Bridge Performance Program, and the National Science Foundation as part of the  
517 CAREER Award titled “Structural Identification to Support Infrastructure Decision-Making.”  
518 Additionally, the authors would like to thank all the participants in the International Bridge  
519 Study who traveled to the bridge and demonstrated technologies and techniques as part of this  
520 research effort and Rutgers CAIT for hosting a summary workshop (<http://cait.rutgers.edu/ibs-2011-agenda>).  
521

522

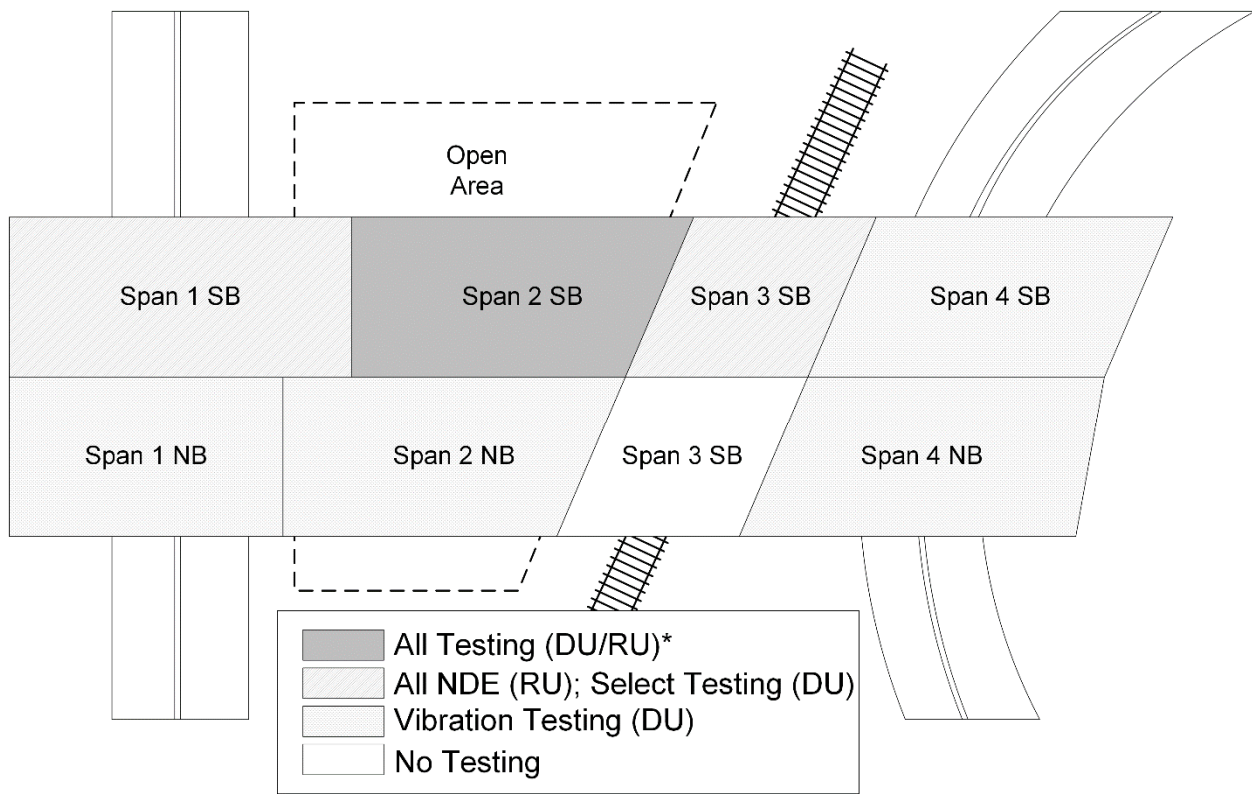
523

524 **References**

- 525 Alampalli, S. (2001). Correlation Between Bridge Vibration and Bridge Deck Cracking: A  
526 Qualitative Study. New York, New York State Department of Transportation. **Report #136:** 50.
- 527
- 528 Beck, J. (2004). "Model Selection Using Response Measurements: Bayesian Probabilistic  
529 Approach." Journal of Engineering Mechanics **130**(2).
- 530
- 531 Beck, J. and L. S. Katafygiotis (1998). "Updating Models and Their Uncertainties: Bayesian  
532 Statistical Framework." Journal of Engineering Mechanics **124**(4): 455-461.
- 533
- 534 Brownjohn, J., et al. (2001). "Civil structure condition assessment by FE model updating:  
535 methodology and case studies." Finite Elements in Analysis and Design **37**: 761-775.
- 536
- 537 Catbas, F. N., et al. (2013). Structural identification of constructed systems : approaches,  
538 methods, and technologies for effective practice of St-Id. Reston, Virginia, American Society of  
539 Civil Engineers.
- 540
- 541 Daniell, W. and J. Macdonald (2007). "Improved finite element modelling of a cable-stayed  
542 bridge through systematic manual tuning." Engineering Structures **29**(3): 358-371.
- 543
- 544 Dubbs, N. and F. L. Moon (2015). "Comparison and Implementation of Multiple Model  
545 Structural Identification Methods." Journal of Structural Engineering.
- 546
- 547 FHWA (2015). "Federal Highway Administration Research and Technology | Long-Term Bridge  
548 Performance Program ". from  
549 <https://www.fhwa.dot.gov/research/tfhrc/programs/infrastructure/structures/ltpb/index.cfm>.
- 550
- 551 Friswell, M. I., et al. (1998). "The Direct Updating of Damping and Stiffness Matrices."  
552 American Institute of Aeronautics and Astronautics Journal **36**(3): 491-493.
- 553
- 554 Friswell, M. I., et al. (2001). "Finite-element model updating using experimental test data:  
555 parametrization and regularization." Philosophical Transactions of the Royal Society A:  
556 Mathematical, Physical and Engineering Sciences **359**(1778): 169-186.
- 557
- 558 Liu, S. and J. Yao (1978). "Structural Identification Concept." ASCE Journal of the Structural  
559 Division. **104**(ST12): 1845-1858.

- 560  
561 Moon, F. L., et al. (2015). "Leveraging Technology for the Assessment of Highway Bridges."  
562 Journal of Bridge Engineering Submitted.
- 563  
564 Pasquier, R. and I. F. C. Smith (2015). "Iterative structural identification framework for  
565 evaluation of existing structures." Engineering Structures: in press.
- 566  
567 Robert-Nicoud, Y., et al. (2005). "Model Identification of Bridges Using Measurement Data."  
568 Computer-Aided Civil and Infrastructure Engineering **20**: 118-131.
- 569  
570 Sigurdardottir, D. and B. Glisic (2014). Uncertainty in determination of neutral axis of a steel  
571 stringer bridge. Safety, Reliability, Risk and Life-Cycle Performance of Structures and  
572 Infrastructures, CRC Press: 2429-2436.
- 573  
574 Su, D., et al. (2011). Monitoring and Visual Inspection of New Jersey Reference Bridges. 5th  
575 International Conference on Structural Health Monitoring of Intelligent Infrastructure, Cancun,  
576 Mexico.
- 577  
578 Veggeberg, K. (2013). Case Studies of Tools Used in Teaching Structural Dynamics. Special  
579 Topics in Structural Dynamics, Volume 6. R. Allemang, J. De Clerck, C. Nieszrecki and A.  
580 Wicks, Springer New York: 225-231.
- 581  
582 Weidner, J. S. (2012). Structural identification of a complex structure using both conventional  
583 and multiple model approaches: xxii, 421 leaves.
- 584  
585 Wenzel, H., et al. (2011). "Life Cycle Analysis Addressing Maintenance and Repair Options and  
586 Its Affections on Remaining Lifetime." ACI Structural Journal **292**.
- 587  
588 Zhang, J., et al. (2013). "Structural health monitoring of a steel stringer bridge with area  
589 sensing." Structure and Infrastructure Engineering **10**(8): 1049-1058.
- 590  
591 Zhou, Y., et al. (2012). Structural Identification Study of International Bridge Based on Multiple  
592 Reference Impact Study. 15th World Conference on Earthquake Engineering. Lisbon, Portugal
- 593  
594 Zhu, D., et al. (2011). "Vibration testing of a steel girder bridge using cabled and wireless  
595 sensors." Frontiers of Architecture and Civil Engineering in China **5**(3): 249-258.
- 596

597 **Figures**



598

599 **Figure 1 - Overall Site Geometry and Layout**

600



601

602 **Figure 2 - Superstructure from South Abutment Looking North**

603

604

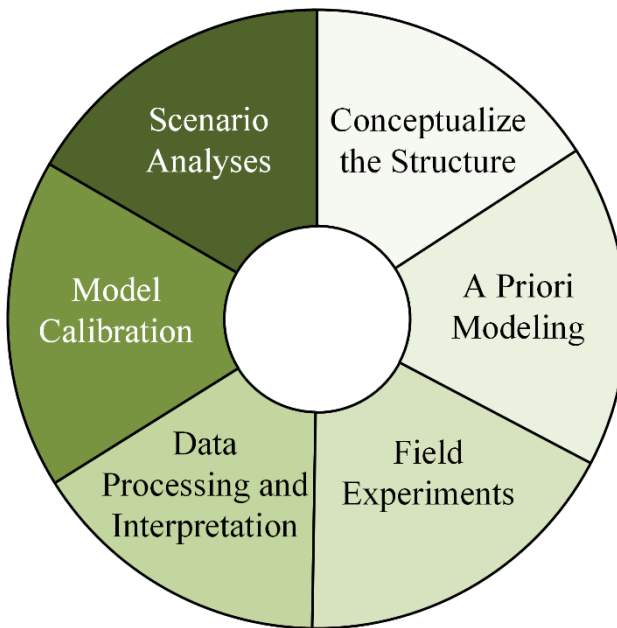
605

606



607

**Figure 3 - Crack in the Span 2 SB Piercap**

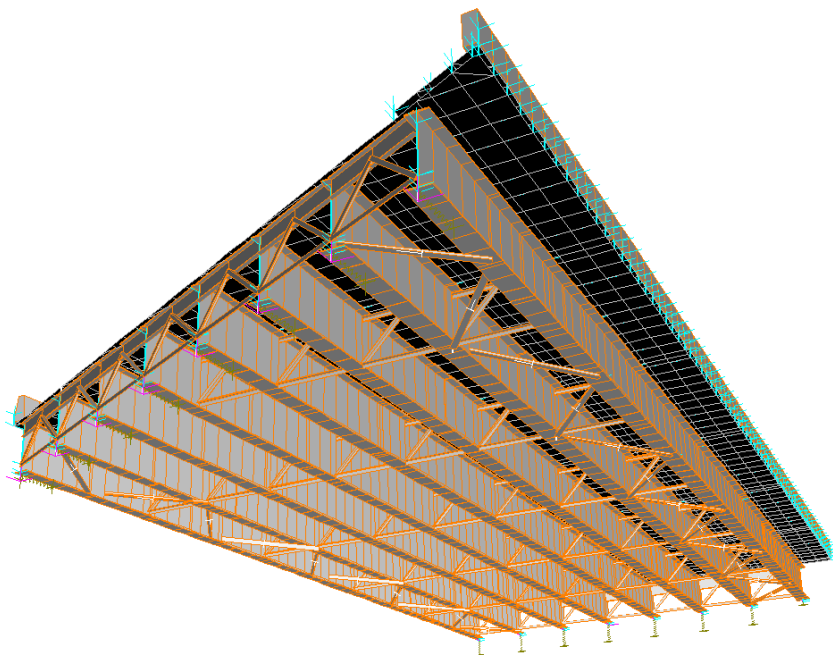


608

609

610

**Figure 4 - Structural Identification**

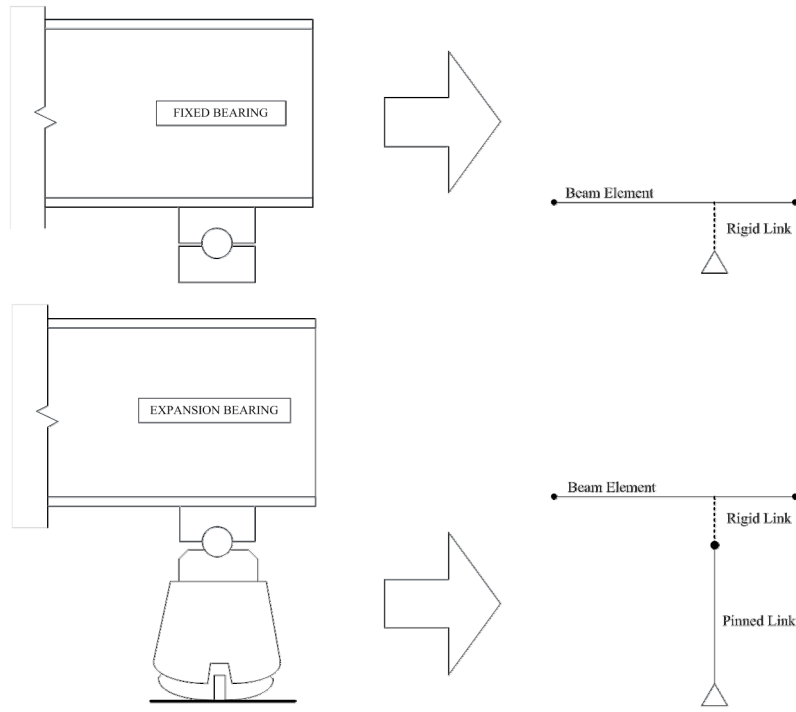


611

612

613

**Figure 5 - Rendering of the A Priori Model**

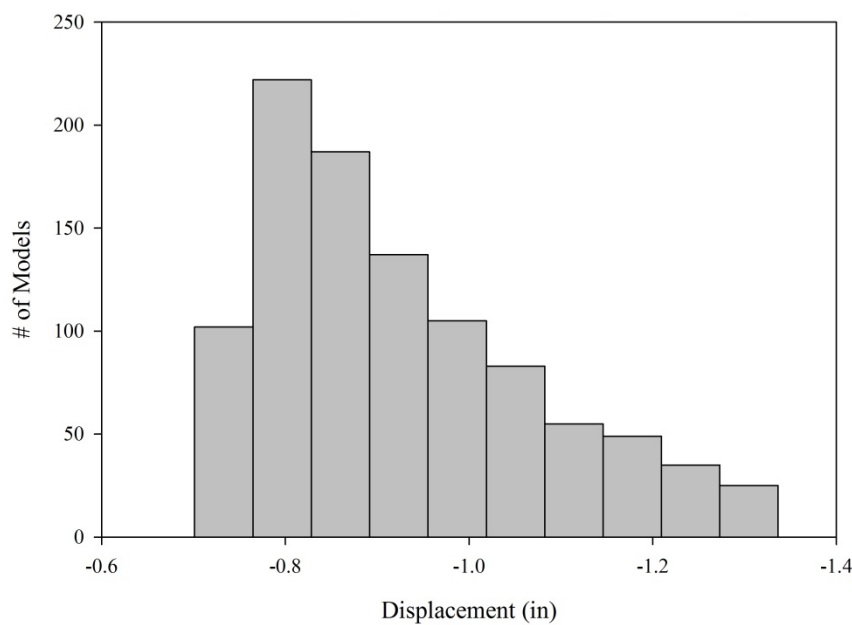


614

615

616

**Figure 6 - Bearing Modeling Details**

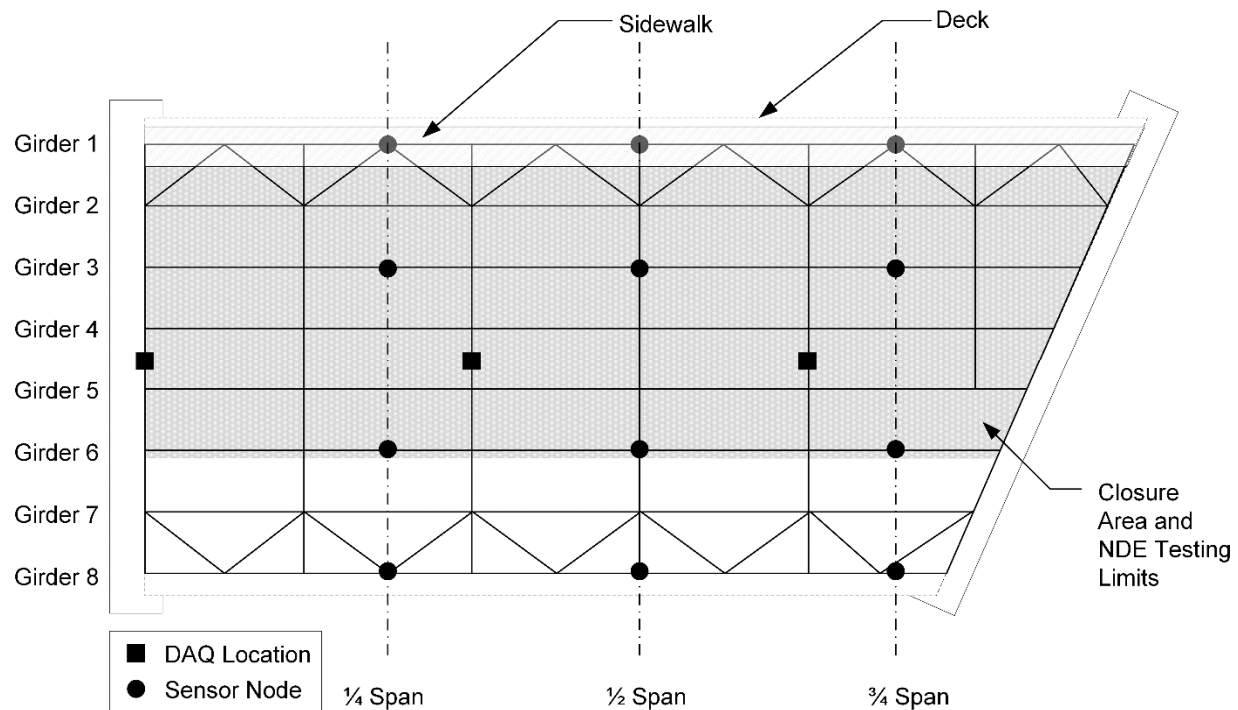


617

618  
619

**Figure 7 – Displacement Response Predictions at Girder #3 from A Priori Model Sensitivity Study**

620

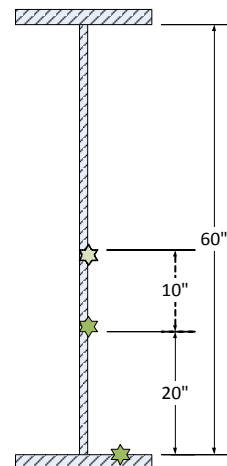


621

622

**Figure 8 - Schematic of the Instrumentation Layout**

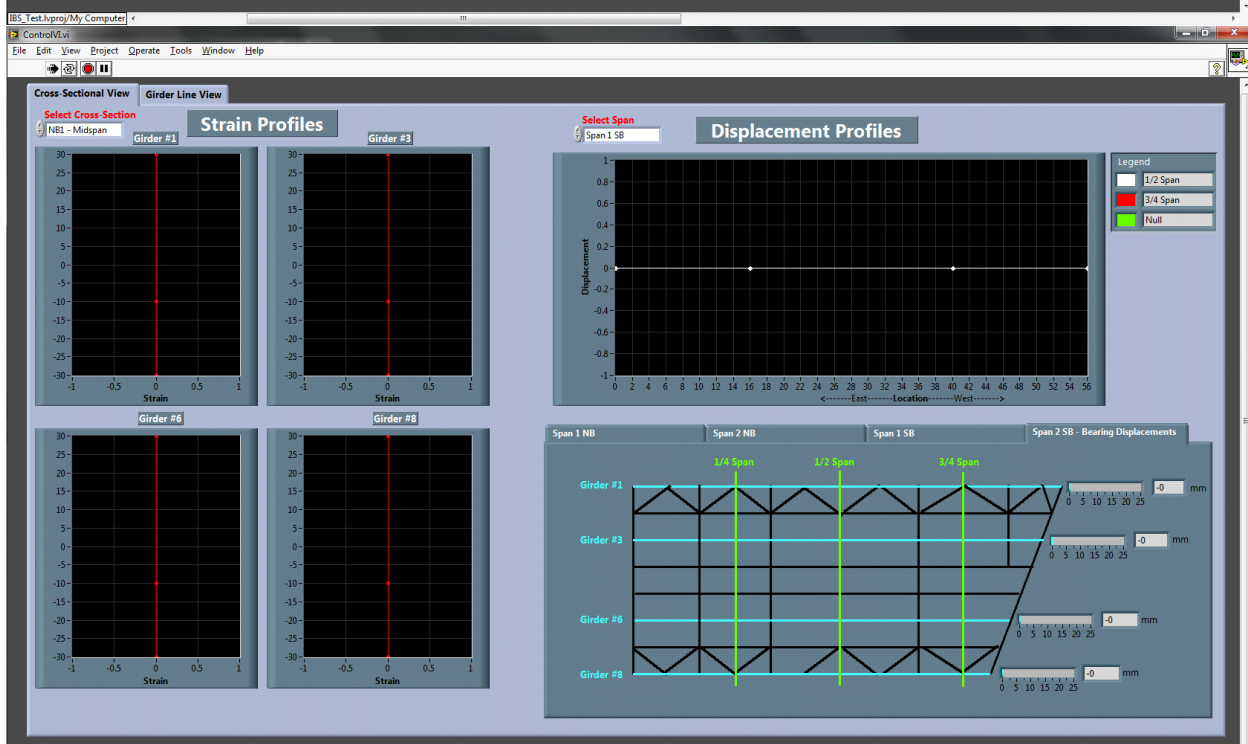
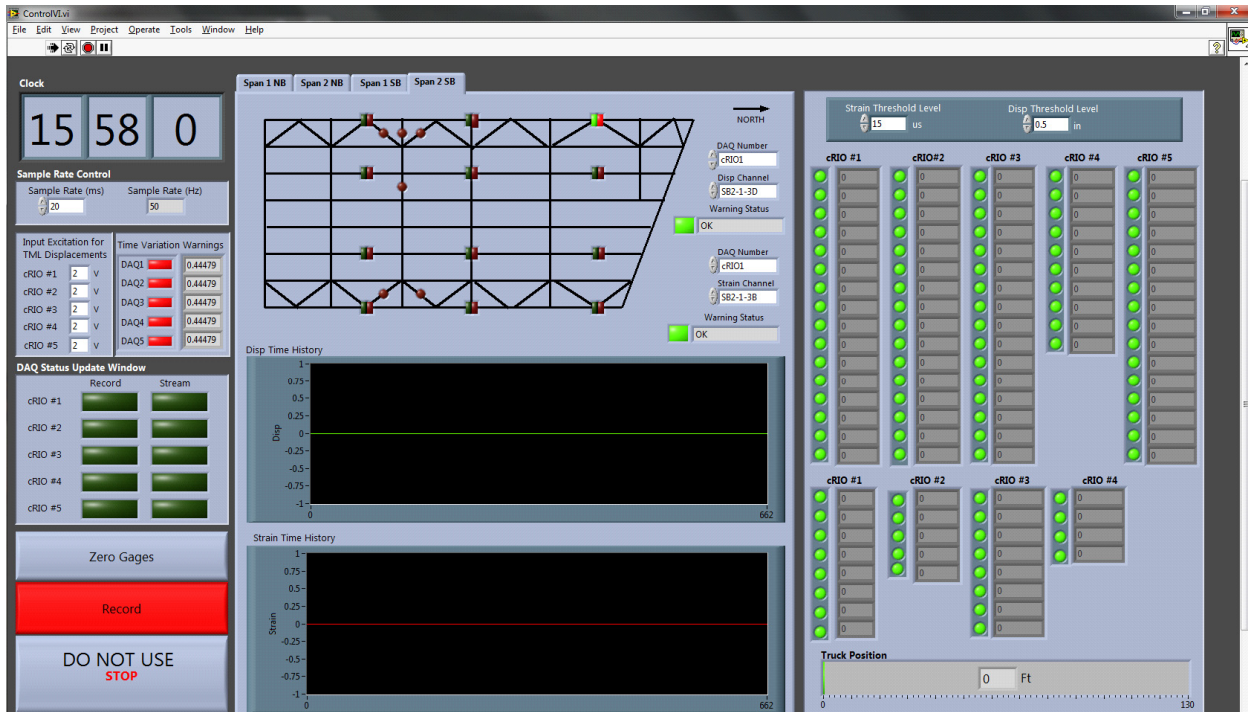
623



624

625

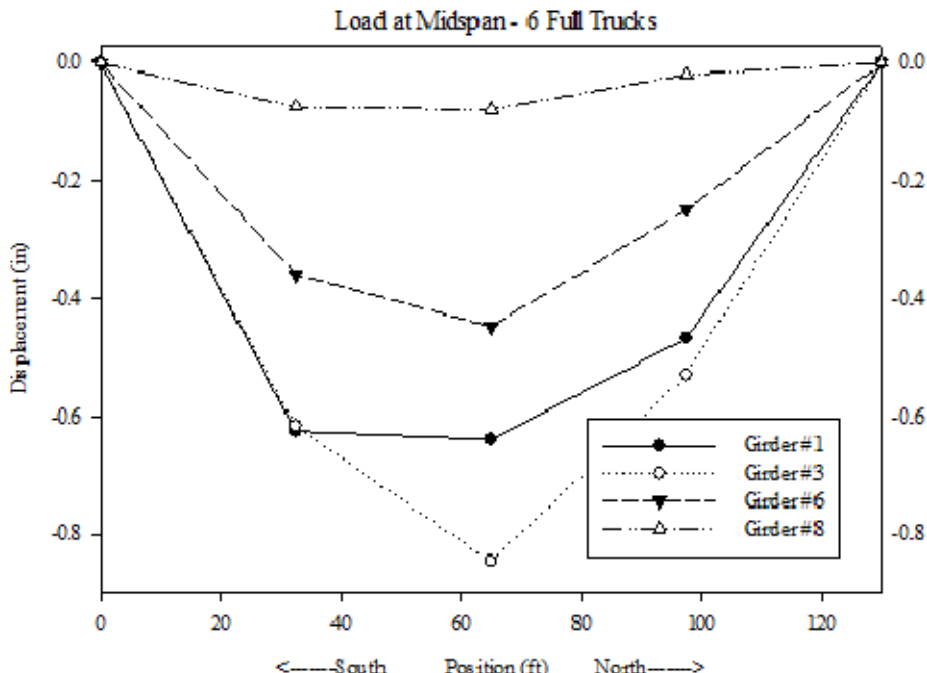
**Figure 9 - Longitudinal Strain Gage Configuration**



628

Figure 10 - Data Visualization Portals

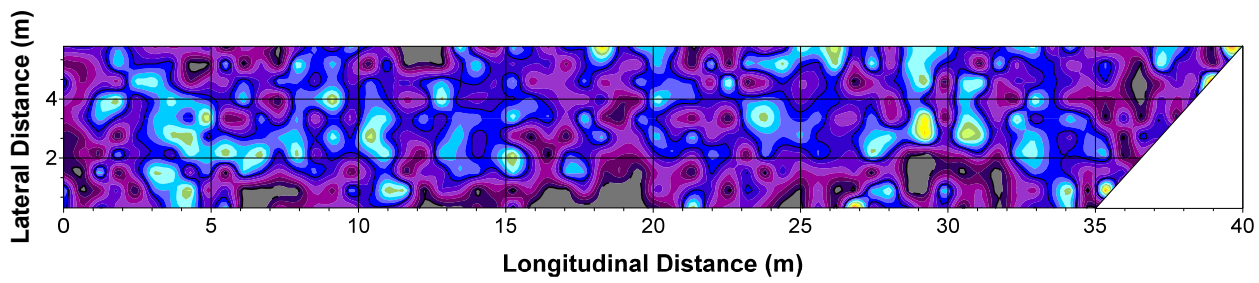
629



630

631

632



633

634

635

636

**Figure 11 - Girder Displacement Profiles**

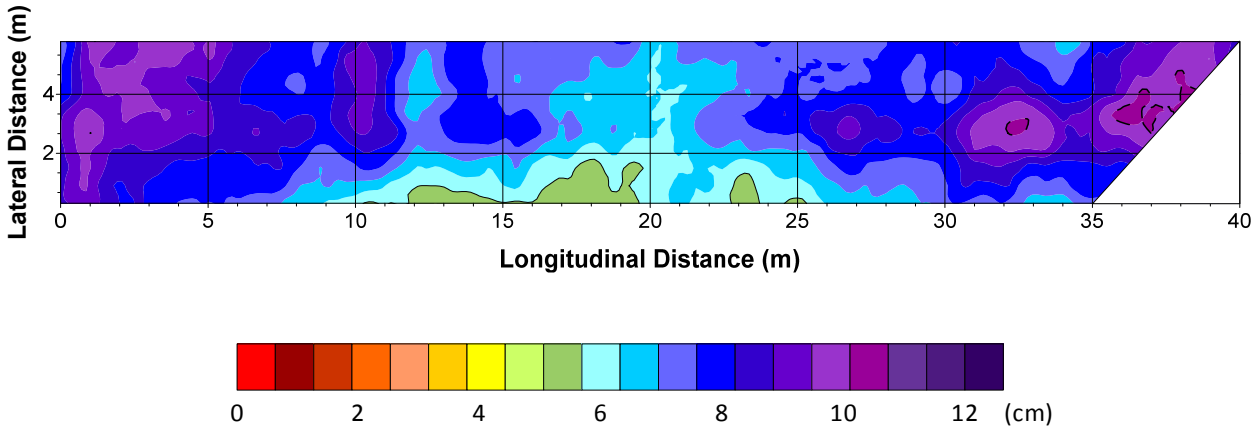


**Figure 13 – Results from Ground Penetrating Radar Testing to Determine Concrete Cover on Span 2 SB.**

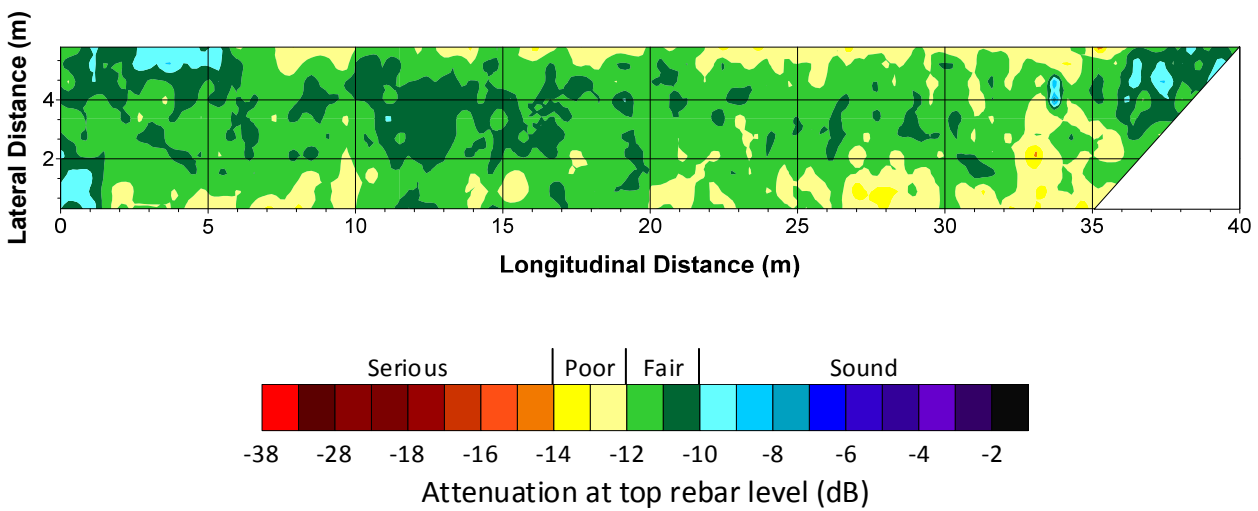
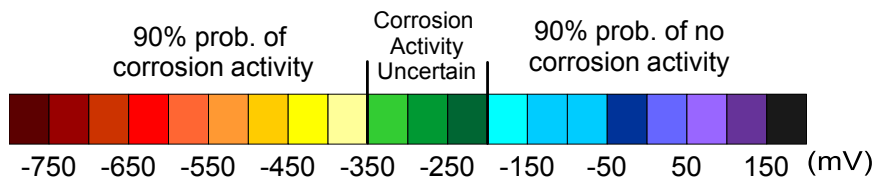
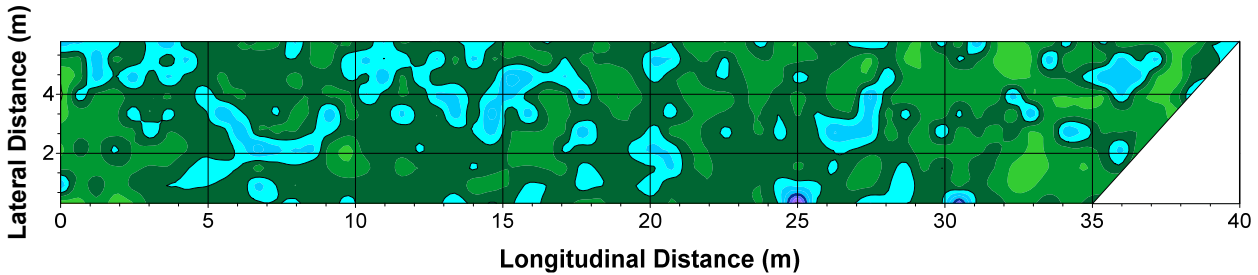
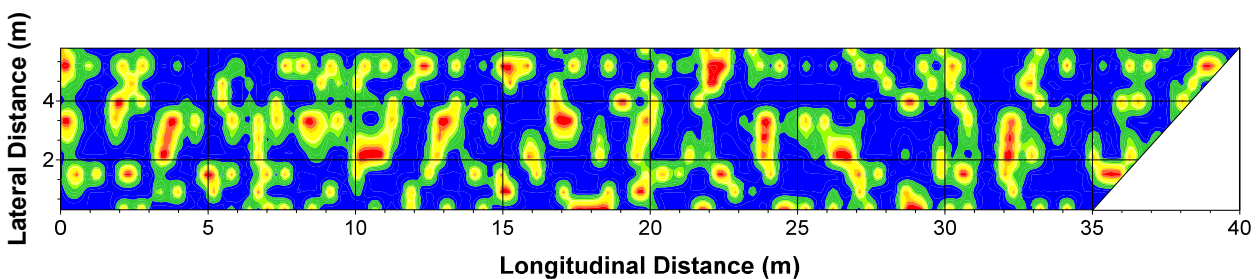


**Figure 14 – Results from Ground Penetrating Radar Testing showing Attenuation at Top Rebar for Span 2 SB**

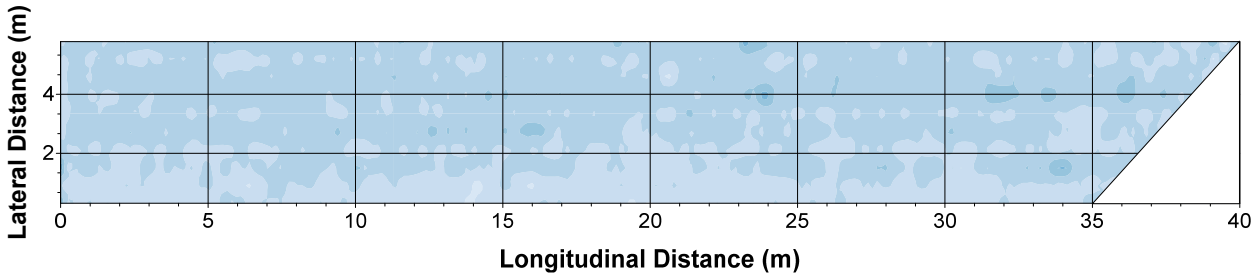


649  
650  
**Figure 15 - Results from Half Cell Potential Testing Showing  
Probability of Corrosion Activity for Span 2 SB**



654  
655  
**Figure 16 - Results from Impact Echo Testing Showing Delaminations for Span 2 SB**

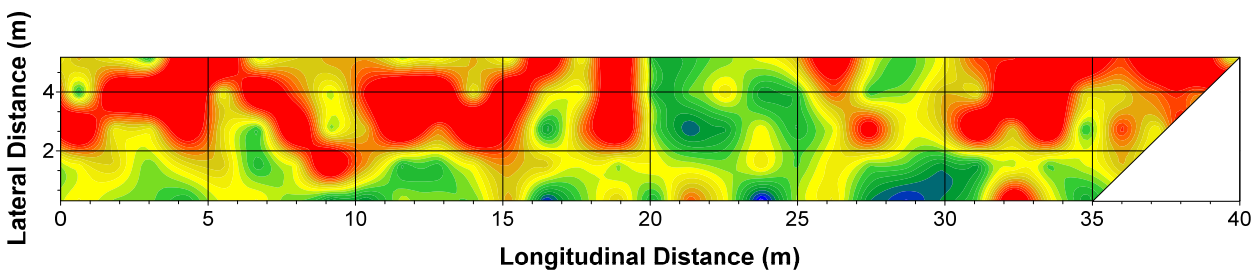
656



658

659      **Figure 17 - Results from MoistScan Testing on Span 2 SB**

660

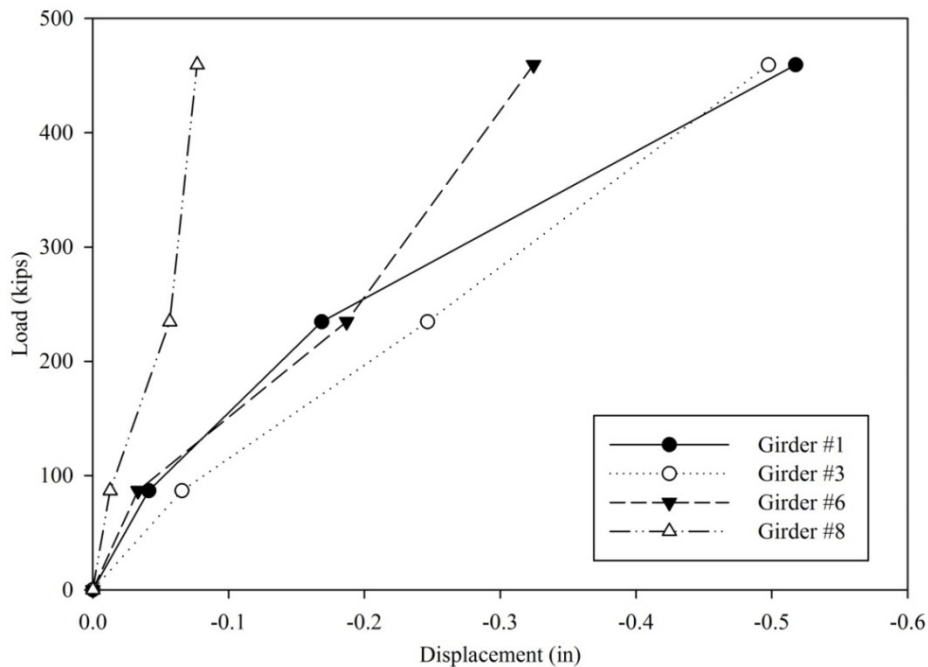


662

663      **Figure 18 - Results from Ultrasonic Surface Wave Testing  
664      Showing Concrete Modulus for Span 2 SB**

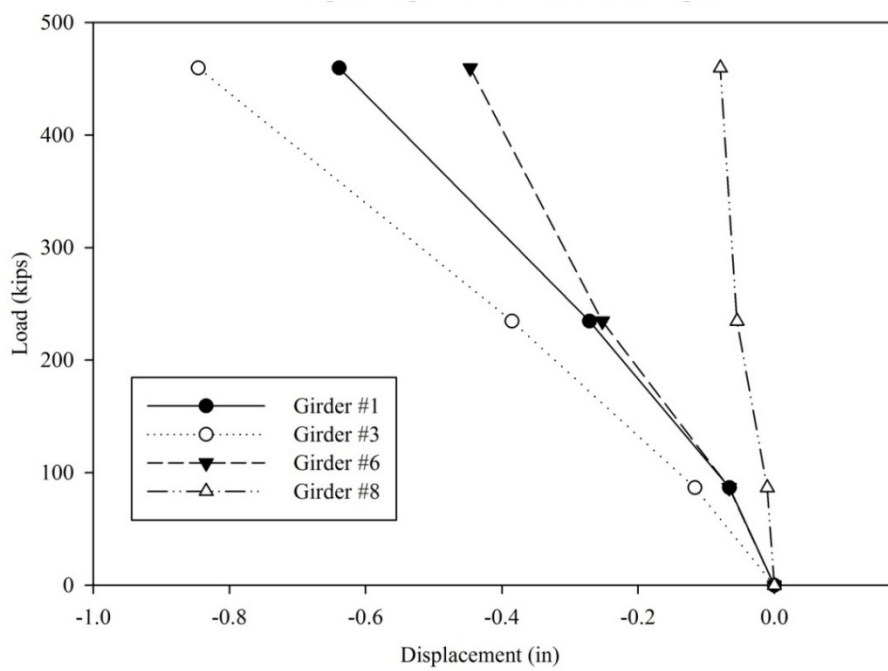
665

666



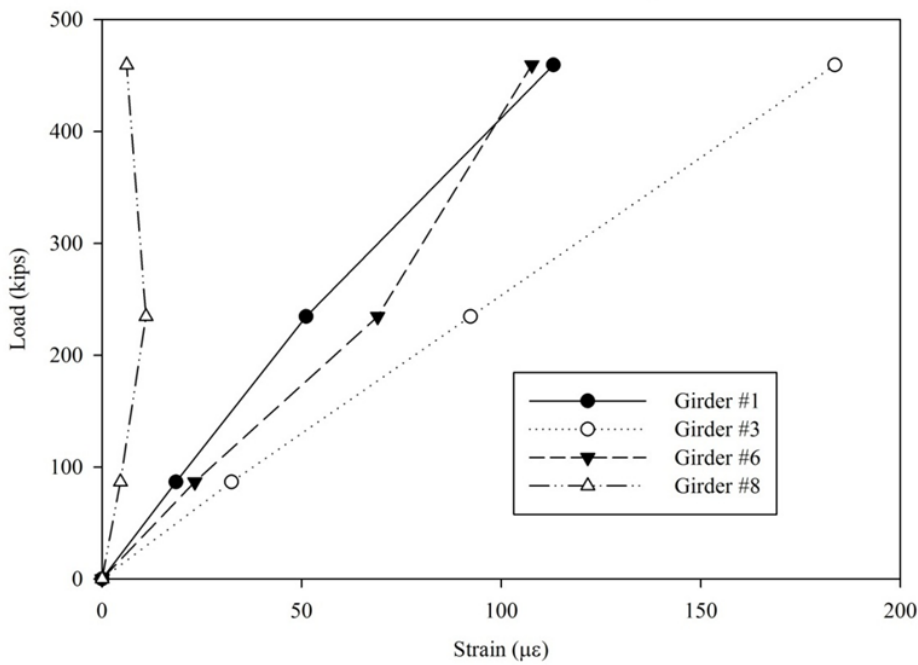
668 **Figure 19 - Quarter Span Displacement - Load at Quarter Span**

669



671 **Figure 20 - Midspan Displacement - Load at Midspan**

672

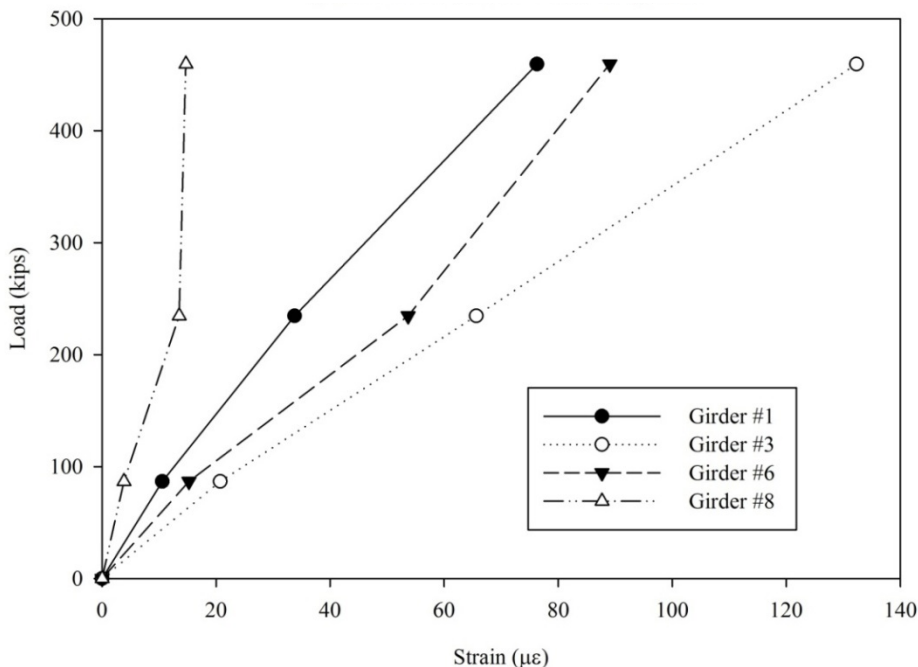


673

674

**Figure 21 - Midspan Strain - Load at Midspan**

675

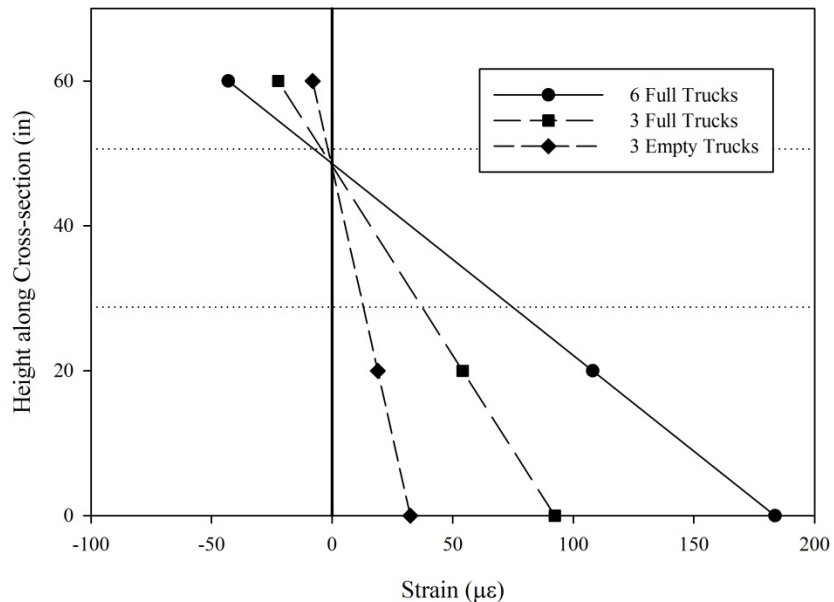


676

677

**Figure 22 - Quarter Span Strain - Load at Quarter Span**

Strain Profile at Midspan of Girder #3 - Load at Midspan

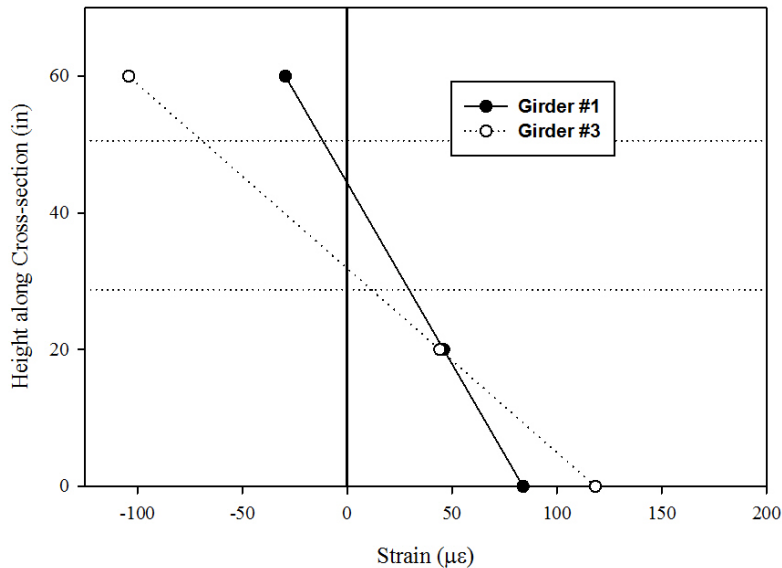


678

679 **Figure 23 - Strain Profile at Midspan of Girder 3 - Load at Midspan**

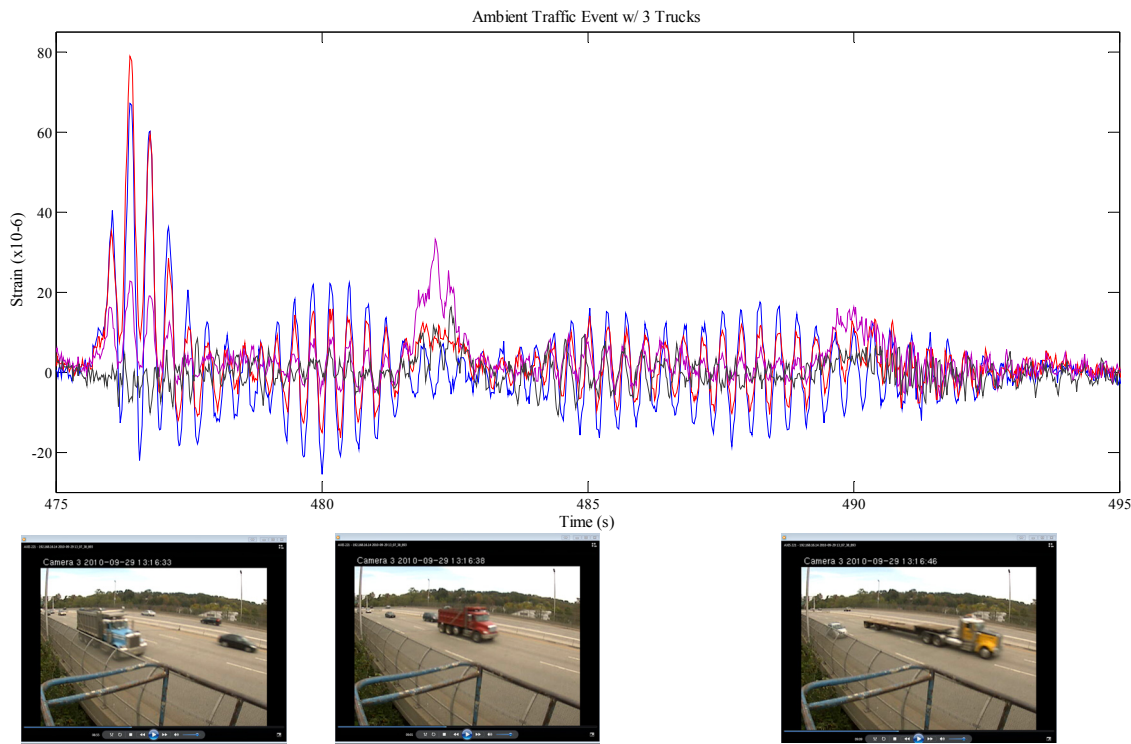
680

Strain Profile at Three Quarter Span of Girder #1 and Girder #3- Full Load



681

682 **Figure 24 - Strain Profile of Girder #1 and #3 at Three Quarter Span with the Max Load at**  
683 **Three Quarter Span**



Truck #1 – Lane 1:  
80us response in Girder #3,  
followed by four vibration  
cycles where Girder #1 shows  
larger response

Truck #2 – Lane 3:  
37us response in Girder #6,  
followed by traffic excitation  
causing 20us response in  
Girder #1

Truck #3 – Lane 3:  
15us response in Girder #6  
which does not excite Girder  
#1 at all

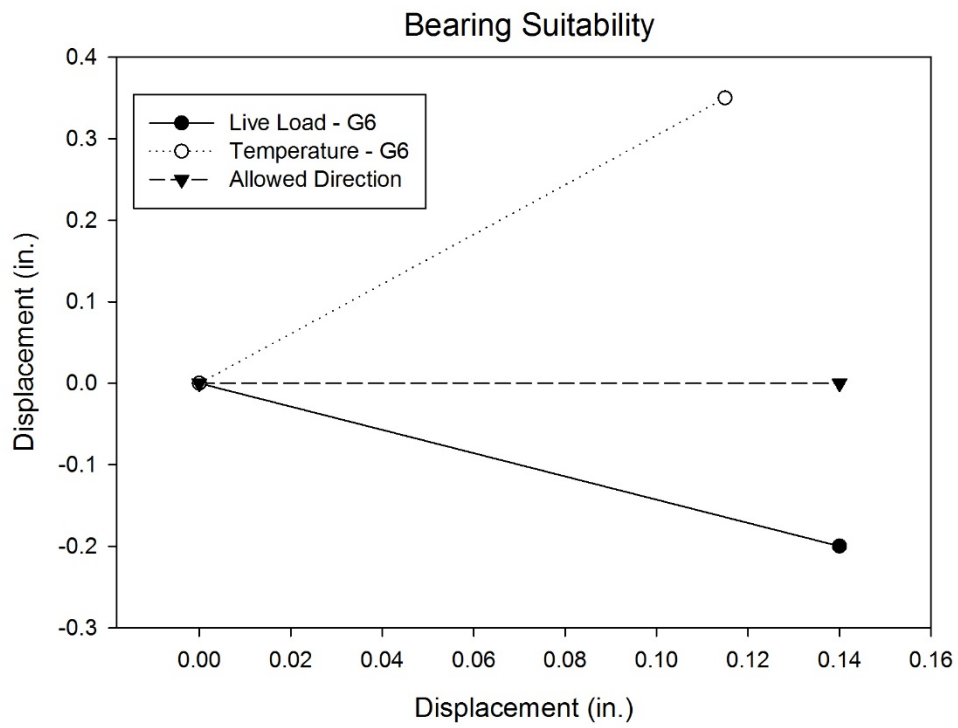
684

685

**Figure 25 – Bridge Strain Time History under Ambient Traffic Including Three Trucks**

686

687



688

689

690

**Figure 26 – Unrestrained Bearing Movement under Various Load Scenarios**

**Table 1 - Addressing Critical Questions Through Data Analysis**

Critical Questions	Test Type	Plot Utilized	Plot Usage
<b>Fatigue cracking and wind bracing details</b>	Static	Wind Bracing Response vs. Truck Position	Member force under static load
	Ambient	Wind Bracing Response - Ambient Traffic	Activation of wind bracing under non-lateral service loads
	Crawl	Diaphragm Response vs. Truck Position	Transverse load distribution
	Ambient	Diaphragm Response - Ambient Traffic	Transverse load distribution - service loads
<b>Pier cap cracking</b>	Ambient	Crack Opening - Service Response	Crack activation under service loads
	Static	Crack Opening vs. Load Level	Linearity of crack opening response
	Static	Girder Displacement vs. Load Level	Linearity of displacement response
	Static	Girder Strain vs. Load Level	Linearity of strain response
<b>Bearing reliability</b>	Static	Bearing Displacement vs. Load Level	Linearity of bearing movement
	Static	Girder Displacement vs. Load Level	Linearity of displacement response
	Static	Strain Response vs. Load Level	Linearity of strain response
	Static	Displacement Basin	Global system response
	Static	Strain Basin	Global system response
<b>Excessive vibration</b>	Static	Composite Action	Neutral axis location
	Ambient	Girder Response - Ambient Traffic	Response under service loads
	Static	Displacement Basin	Global system response
	Static	Girder Strain vs. Load Level	Linearity of strain response
<b>Deck cracking</b>	Static	Composite Action	Neutral axis location

693

694

**Table 2 - Bounds for Parameter Variation – Sensitivity Study (Later Expanded)**

	Lower Bound	Upper Bound
Stiffness Modification Factor of Cross Bracing	0.5	1.2
Composite Action Stiffness (kip/in)	1	100
Rotational Spring Stiffness Rigidity Factor	0	1

695

696

697

**Table 3 - Measured Peak Strain and Displacement Responses**

Span-Girder-Location	Strain ( $\times 10^{-6}$ )	Disp. (in.)
SB2-1-3/4	83.9	-0.467
SB2-1-1/2	113.1	-0.639
SB2-1-1/4	86.2	-0.625
SB2-3-3/4	133.7	-0.530
<b>SB2-3-1/2</b>	<b>183.6</b>	<b>-0.846</b>
SB2-3-1/4	132.3	-0.616
SB2-6-3/4	70.4	-0.249
SB2-6-1/2	107.7	-0.447
SB2-6-1/4	89.0	-0.358
SB2-8-3/4	10.1	-0.024
SB2-8-1/2	12.6	-0.085
SB2-8-1/4	17.4	-0.077

698

699

700  
701**Table 4 - Comparison of Measured Responses with Manually and Automatically Calibrated Model Output**

Location	Displacement Comparisons			Strain Comparisons		
	Measured (in.)	Manually Calibrated Model (in.)	Automatically Calibrated Model (in.)	Measured ( $\times 10^{-6}$ )	Manually Calibrated Model ( $\times 10^{-6}$ )	Automatically Calibrated Model ( $\times 10^{-6}$ )
G1-1/4	-0.625	-0.598	-0.561	86.2	88.5	65.7
G3-1/4	-0.616	-0.651	-0.645	111.9	102.9	82.8
G6-1/4	-0.358	-0.387	-0.365	77.4	78.3	57.0
G8-1/4	-0.075	-0.104	-0.078	15.7	43.9	24.5
G1-2/4	-0.639	-0.700	-0.661	113.1	123.0	101.6
G3-2/4	-0.846	-0.836	-0.848	183.6	193.1	172.7
G6-2/4	-0.447	-0.457	-0.439	107.7	112.5	91.9
G8-2/4	-0.079	-0.104	-0.069	6.2	35.2	17.6
G1-3/4	-0.467	-0.513	-0.479	83.9	79.6	59.7
G3-3/4	-0.530	-0.567	-0.555	118.4	107.9	79.8
G6-3/4	-0.249	-0.247	-0.229	70.4	58.8	27.2
G8-3/4	-0.019	-0.024	-0.020	5.0	19.0	5.0

702

703

**Table 5 - Final Parameter Values from Manual and Automated Model Calibration**

Parameter	Manual Calibration	Parameter ID
Material Properties		
$E_{Deck}$	3122 ksi	3122 ksi
$E_{Girders}$	29000 ksi	29000 ksi
$E_{parapet}$	3500 ksi	3326 ksi
$E_{Barrier}$	4000 ksi	3413 ksi
Composite Action Stiffness		
CompAct 1	10000 kip/in	574 kip/in
CompAct 2	1000 kip/in	574 kip/in
CompAct 3	100 kip/in	574 kip/in
Bearing Stiffness		
$k_v$ (G1)	50 kip/in	27 kip/in
$k_v$ (others)	Fixed	692 kip/in
$k_L$ (G1,G8)	350 kip/in	699 kip/in
$k_L$ (others)	100 kip/in	699 kip/in
$k_T$ (all)	10 kip/in	10 kip/in

704

705

**Table 6 - Calibration Results from Parameter Identification using only Strains**

Location	Displacement Comparisons			Strain Comparisons		
	Measured (in.)	Automatically Calibrated Model (in.)	Difference	Measured (x 10 <sup>-6</sup> )	Automatically Calibrated Model (x 10 <sup>-6</sup> )	Difference
G1-1/4	-0.625	-0.499	0.126	86.2	62.2	-24.0
G3-1/4	-0.616	-0.618	-0.002	111.9	78.4	-33.5
G6-1/4	-0.358	-0.355	0.003	77.4	55.5	-21.9
G8-1/4	-0.075	-0.076	-0.001	15.7	22.9	7.3
G1-2/4	-0.639	-0.604	0.035	113.1	98.9	-14.2
G3-2/4	-0.846	-0.798	0.048	183.6	167.9	-15.7
G6-2/4	-0.447	-0.417	0.030	107.7	89.4	-18.3
G8-2/4	-0.079	-0.069	0.010	6.2	16.9	10.7
G1-3/4	-0.467	-0.440	0.027	83.9	57.3	-26.5
G3-3/4	-0.530	-0.519	0.011	118.4	76.1	-42.3
G6-3/4	-0.249	-0.215	0.034	70.4	23.5	-46.8
G8-3/4	-0.019	-0.020	-0.001	5.0	4.3	-0.6

706

707

708

**Table 7 - Inventory Ratings for Girder #4 at Midspan under a Single Truck**

Instance	RF
Inspection	1.90
Original	2.86
Manual	3.54
Static	3.58
Dynamic	2.99

709

710

711